

Predicting Intraocular Pressure using Neural Networks: Incorporating Eye Fundus Images and Clinical Data from PAPILA Dataset

Fernando Ly Yang^{1*}, Chou M¹, Lauren Van Lancker¹, Chris Panos¹

Abstract

Importance: Glaucoma, a leading cause of irreversible blindness, necessitates accurate intraocular pressure (IOP) prediction for early detection and management. The integration of deep learning algorithms with clinical data presents a novel approach to enhance diagnostic accuracy and patient care in ophthalmology, addressing a critical gap in current diagnostic methodologies.

Objective: To assess the effectiveness of deep learning models, specifically Segformer and EfficientNetV2B0, in predicting IOP when combined with clinical data and eye fundus images, aiming to improve diagnostic accuracy and management of glaucoma.

Design, Setting, and Participants: This cross-sectional study utilized the PAPILA database. The study employed publicly available databases G1020, ORIGA, and PAPILA, incorporating retinal fundus images from patients diagnosed with glaucoma. It focused on leveraging clinical data such as central corneal thickness, age, gender, axial length, and refractive defect for predictive analysis.

Exposure(s): Participants were exposed to deep learning algorithm-based analysis, integrating clinical data with retinal fundus images to predict IOP.

Main Outcome(s) and Measure(s): The primary outcome was the accuracy of the IOP predictions, evaluated using Mean Absolute Error (MAE), Coefficient of Determination (R-squared), and Root Mean Squared Error (RMSE). The model's performance was assessed based on its ability to accurately predict actual measured IOP values.

Results: The study analyzed images and clinical data from patients within the PAPILA database. The deep learning model achieved an MAE of 2.52, indicating moderate accuracy in predicting IOP. The R-squared value was reported at 0.10, reflecting the model's limited capacity to explain variance in IOP values among the study population.

Conclusions and Relevance: The findings suggest that deep learning algorithms, when integrated with clinical data, have the potential to predict IOP with a moderate level of accuracy. This innovative approach could significantly impact the management and diagnosis of glaucoma. This study underscores the potential of AI in revolutionizing ophthalmic diagnostics, particularly for glaucoma, although further validation and improvement of these models are necessary before clinical application.

Affiliation:

¹Epsom and St Helier University Hospitals NHS Trust, Glaucoma, Carshalton, United Kingdom

*Corresponding author:

Fernando Ly Yang, Epsom and St Helier University Hospitals NHS Trust, Glaucoma, Carshalton, United Kingdom.

Citation: Fernando Ly Yang, Chou M, Lauren Van Lancker, Chris Panos. Predicting Intraocular Pressure using Neural Networks: Incorporating Eye Fundus Images and Clinical Data from PAPILA Dataset. Journal of Bioinformatics and Systems Biology. 8 (2025): 38-42.

Received: April 19, 2025

Accepted: April 24, 2025

Published: May 05, 2025

Keywords: Glaucoma; Eye; IOP;

Introduction

The simultaneous maturation of several pivotal digital innovations in information and communications technology has surged at an unprecedented pace in this new century. This rapid evolution has reverberated across all sectors, including healthcare. Notable digital advancements, such as the further integration of telehealth services, the advent of 5th generation wireless networks (5G), artificial intelligence (AI) methodologies like machine learning (ML) and deep learning (DL), and the widespread adoption of the Internet of Things (IoT), alongside fortified digital security capabilities such as blockchain, have cultivated an extraordinary landscape ripe with new prospects in healthcare and beyond [1].

Glaucoma is known as the major cause of irreversible blindness worldwide [2,3].

The global prevalence of glaucoma is projected to rise to 111.8 million by 2040, with a disproportionate impact on individuals living in Asia and Africa [4]. Undiagnosed glaucoma cases still account for more than 50 % of the cases worldwide [5]. These projections are crucial for shaping the development of glaucoma screening, treatment, and associated public health initiatives.

Materials & Methods

In this study, the public databases G1020 [6], ORIGA[7], and PAPILA[8] were employed. G1020 and Origa, containing a combined total of 1670 images, were utilized for training a Segformer model (nvidia/mit-b0) from HuggingFace [9], aimed at segmenting the optic disc. Sixty percent of the 1670 images were designated for training, with 20% allocated for validation and another 20% for testing. Validation results revealed an overall accuracy of 99%, with a loss of 1%, while during training, the overall accuracy was 98%, with a loss of 3%. Following this, the transformer model was applied to segment the PAPILA[8] dataset and to crop the optic nerve at 1.5 diameters of the optic disc, covering the upward, downward, leftward, and rightward directions.

The PAPILA [8] dataset encompasses three diagnoses—normal, glaucoma, and uncertain. The uncertain diagnoses were excluded from analysis, resulting in a total of 331 images, consisting of 298 normal images and 33 glaucoma images. Clinical data associated with these images, such as the diagnosis of glaucoma, central corneal thickness, age, gender, axial length, and refractive defect, were utilized to predict intraocular pressure. For this purpose, 70% of the images were employed for training, while 15% each were allocated for validation and testing.

Fine-tuning of EfficientNetV2B0 [10] involved utilizing the last 200 layers with images, employing AdamW optimizer with a learning rate of 1e-2 and weight decay of 1e-4, and utilizing mean square error as the loss function. Subsequently, image features were concatenated with metadata features to facilitate the prediction of intraocular pressure.

Results

With the Segformer neural network, the entire PAPILA [8] dataset was cropped (Figure 1). Uncertain diagnoses from the PAPILA [8] dataset were excluded. Among the dataset, 90% of the images were labeled as normal, while 10% were identified as having glaucoma. The distribution of gender within the dataset consisted of 34% men and 66% women. The mean age was 59 years with a standard deviation of 12. The mean refractive error was 0.85 with a standard deviation of 2.11. The mean central corneal thickness was 534 with a standard deviation of 41. Additionally, the mean axial length was 23.46 with a standard deviation of 1.10, and the mean intraocular pressure (IOP) was 16.01 with a standard deviation of 3.35. The majority of IOP observations are concentrated in the range of 13.0 to 20.0, with the highest frequency observed at an IOP value of 16.0. There are fewer observations with IOP values above 20.0, indicating that higher IOP values are less common in the dataset (Figure 2).

The PAPILA [8] dataset images, along with the clinical variables mentioned above, were utilized to train a neural network for predicting intraocular pressure (IOP). The dataset was split into three subsets: 70% for training, 15% for validation, and 15% for testing purposes. The outcomes of the neural network model on the test subset are depicted in Figures 3 and 4.

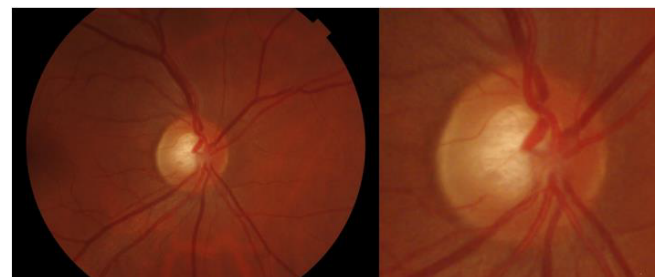


Figure 1: Shows a comparison of normal original PAPILA dataset image and the cropped One.

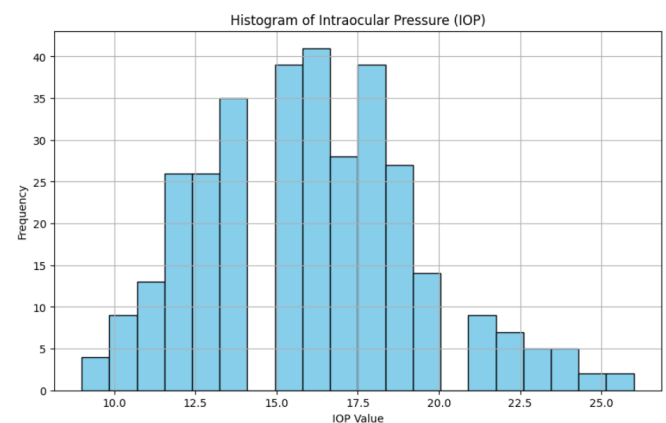


Figure 2: Histogram illustrating intraocular pressure distribution in PAPILA dataset

| | test | prediction | | test | prediction | | test | prediction |
|----|------|----------------------|----|------|----------------------|----|------|----------------------|
| 0 | [15] | [14.944922835542963] | 11 | [16] | [14.246726989027675] | 21 | [19] | [18.029272309247194] |
| 1 | [12] | [15.274864525626509] | 12 | [11] | [15.436266249229288] | 22 | [20] | [17.148059385273477] |
| 2 | [11] | [15.166125203786926] | 13 | [14] | [14.064854090131815] | 23 | [14] | [18.330019127484753] |
| 3 | [19] | [17.108521837834296] | 14 | [17] | [16.373629367281556] | 24 | [19] | [18.354207979728063] |
| 4 | [14] | [16.95802165465424] | 15 | [19] | [17.378559220638664] | 25 | [13] | [15.755470136172349] |
| 5 | [13] | [16.976082290932958] | 16 | [12] | [15.144685230753582] | 26 | [12] | [17.71958646424694] |
| 6 | [13] | [14.580154413731996] | 17 | [21] | [19.67217721837627] | 27 | [18] | [20.516567948755398] |
| 7 | [16] | [19.227385556174003] | 18 | [17] | [16.921364779253576] | 28 | [15] | [16.149622587167762] |
| 8 | [17] | [16.009650999814475] | 19 | [18] | [15.5392558705319] | 29 | [15] | [16.18061101587358] |
| 9 | [18] | [16.745384716137274] | 20 | [16] | [19.42625320555545] | 30 | [16] | [16.10622227021653] |
| 10 | [18] | [16.01803126212299] | | | | | | |

Figure 3: Displays a comparison between the first thirty intraocular pressure predictions generated by the neural network and the corresponding real intraocular pressure values from the test subset of the PAPILA dataset.

| | test | prediction | | test | prediction |
|----|------|----------------------|----|------|----------------------|
| 31 | [18] | [16.91193381292293] | 41 | [15] | [17.22250516922057] |
| 32 | [14] | [15.166880227135255] | 42 | [12] | [15.130751928303633] |
| 33 | [20] | [19.02615928692562] | 43 | [21] | [13.978606775321035] |
| 34 | [16] | [15.451944777810244] | 44 | [21] | [15.46749151356265] |
| 35 | [24] | [17.30209157610856] | 45 | [11] | [17.365196853153527] |
| 36 | [14] | [15.504738018836207] | 46 | [18] | [14.610262901972094] |
| 37 | [22] | [16.296525242686073] | 47 | [20] | [16.705234979466308] |
| 38 | [10] | [15.283677480955339] | 48 | [14] | [13.464821717935479] |
| 39 | [19] | [15.702072133690164] | 49 | [16] | [16.20478947926864] |
| 40 | [21] | [19.724818064534034] | | | |

Figure 4: Illustrates a comparison between the remaining cases of intraocular pressure predictions generated by the neural network and the corresponding real intraocular pressure values from the test subset of the PAPILA dataset.

The Mean Absolute Error (MAE) of the model is 2.52, indicating an average absolute deviation of approximately 2.52 units between the predicted and actual values. The Coefficient of Determination (R-squared) value of 0.10 suggests that only around 10.24% of the variance in the target variable is explained by the model. The Root Mean Squared Error (RMSE) is 3.13, which represents the square root of the average of squared differences between predicted and actual values, indicating an average deviation of approximately 3.13 units from the actual values.

Discussion

Many studies have been published demonstrating neural networks' capability to accurately classify glaucoma and normal patients using retinal fundus images, with AUC values typically around 99% [11-14]. However, this study represents the first attempt to predict intraocular pressure (IOP) using retinal fundus images in combination with ophthalmology clinical data. Another study by Isshi K et al. [15] attempted to predict IOP using machine learning models based solely on systemic variables, but their results were found to be

insufficient when compared to predicting IOP using only retinal fundus images.

In our study, we trained a deep learning algorithm using both eye fundus images and eye clinical data, in contrast to Isshi K et al [15], who trained machine learning algorithms solely with systemic variables. Our Mean Absolute Error (MAE) of 2.52 is very similar to his MAE of 2.29. This metric is highly clinically interpretable. When the MAE is 2 and the predicted result is 15, it means that, on average, the model's predictions deviate by approximately 2 units from the actual values.

Thus, if the predicted result is 15 with an MAE of 2, we can reasonably expect the actual value to fall within the range of 13 to 17. This interpretation stems from the fact that the MAE represents the average absolute deviation of the model's predictions from the actual values. Therefore, the MAE provides an estimate of the typical magnitude of errors made by the model. With an MAE of 2, it suggests that the majority of actual values would likely fall within ± 2 units of the predicted value of 15.

Our deep learning model achieved an R-squared value of 0.1, which is comparable to the R-squared value of Isshi K et al [15], who rounds it to 0.15 depending on the machine learning model employed. However, it's crucial to understand that R-squared is not an ideal metric for evaluating non-linear models like deep learning models [16,17]. Therefore, even if a deep learning model performs well in terms of prediction accuracy, its R-squared value may not reflect this accurately.

While eye fundus images contain a wealth of information that can be leveraged to predict age [18,19], vascular risk factors [18,19], sex [20], and even neurological diseases such as Alzheimer's [21,2], it lacks sufficient information to predict intraocular pressure (IOP) [8] on its own. Additional clinical data must be incorporated to accurately predict IOP.

Using deep learning to predict IOP could be useful if employed in conjunction with other neural networks that distinguish between glaucoma and healthy individuals. By doing so, in locations lacking access to ophthalmology resources, a network that distinguishes between healthy and glaucomatous eyes, combined with another network that estimates IOP, could establish protocols and different criteria for referral.

Conclusions

In summary, our research demonstrates the potential of combining deep learning algorithms with clinical data to predict intraocular pressure (IOP). This innovative approach offers opportunities to optimize diagnostic protocols and improve patient management strategies, particularly in areas with limited access to ophthalmic resources.

Meeting presentation: Accepted in European Glaucoma Congress 2024

Financial support: None

Conflict of interest: No conflict of interest exists for any author.

References

- Li JO, Liu H, Ting DSJ, et al. Digital technology, telemedicine, and artificial intelligence in ophthalmology: A global perspective. *Prog Retin Eye Res* 82 (2021): 100900.
- Yadav KS, Rajpurohit R, Sharma S. Glaucoma: Current treatment and impact of advanced drug delivery systems. *Life Sci* 221 (2019): 362-376.
- Gupta P, Yadav KS. Applications of microneedles in delivering drugs for various ocular diseases. *Life Sci* 237 (2019): 116907.
- Tham YC, Li X, Wong TY, et al. Global prevalence of glaucoma and projections of glaucoma burden through 2040: a systematic review and meta-analysis. *Ophthalmology* 121 (2014): 2081-2090.
- Gupta P, Zhao D, Guallar E, et al. Prevalence of Glaucoma in the United States: The 2005-2008 National Health and Nutrition Examination Survey. *Invest Ophthalmol Vis Sci* 57 (2016): 2905-2913.
- Bajwa MN, Singh GAP, Neumeier W, et al. G1020: A Benchmark Retinal Fundus Image Dataset for Computer-Aided Glaucoma Detection. *IJCNN* (2020): 1-7.
- Zhang Z, Yin FS, Liu J, et al. ORIGA(-light): an online retinal fundus image database for glaucoma analysis and research. *Annu Int Conf IEEE Eng Med Biol Soc* 2010 (2010): 3065-8.
- Kovalyk O, Morales-Sánchez J, Verdú-Monedero R, et al. PAPILA: Dataset with fundus images and clinical data of both eyes of the same patient for glaucoma assessment. *Sci Data* 9 (2022): 291.
- Hugging Face. Hugging Face Model Hub (2020).
- Keras. EfficientNetV2B0 (2021).
- Velpula VK, Sharma LD. Multi-stage glaucoma classification using pre-trained convolutional neural networks and voting-based classifier fusion. *Front Physiol* 14 (2023): 1175881.
- Ganesh SS, Kannayeram G, Karthick A, et al. A Novel Context Aware Joint Segmentation and Classification Framework for Glaucoma Detection. *Comput Math Methods Med* 2021 (2021): 2921737.
- Rehman AU, Taj IA, Sajid M, Karimov KS. An ensemble framework based on Deep CNNs architecture for glaucoma classification using fundus photography. *Math Biosci Eng* 18 (2021): 5321-5346.
- Hemelings R, Elen B, Schuster AK, et al. A generalizable deep learning regression model for automated glaucoma screening from fundus images. *NPJ Digit Med* 6 (2023): 112.
- Ishii K, Asaoka R, Omoto T, et al. Predicting intraocular pressure using systemic variables or fundus photography with deep learning in a health examination cohort. *Sci Rep* 11 (2021): 3687.
- Miaou SP, Lu A, Lum HS. Pitfalls of using R-squared to evaluate goodness of fit of accident prediction models. *Transportation Research Record* 1542 (1996): 6-13.
- Bates DM, Watts DG. Nonlinear regression analysis and its applications. New York, NY: John Wiley & Sons (1988).
- Zhu Z, Chen Y, Wang W, et al. Association of retinal age gap with arterial stiffness and incident cardiovascular disease. *Stroke* 53 (2022): 3320-3328.

19. Zhu Z, Hu W, Chen R, et al. Retinal age gap as a predictive biomarker of stroke risk. *BMC Med* 20 (2022): 466.
20. Korot E, Pontikos N, Liu X, et al. Predicting sex from retinal fundus photographs using automated deep learning. *Sci Rep* 11 (2021): 10286.
21. Costanzo E, Lengyel I, Parravano M, et al. Ocular biomarkers for Alzheimer disease dementia: An umbrella review of systematic reviews and meta-analyses. *JAMA Ophthalmol* 141 (2023): 84-91.
22. Armstrong GW, Kim LA, Vingopoulos F, et al. Retinal imaging findings in carriers with PSEN1-associated early-onset familial Alzheimer disease before onset of cognitive symptoms. *JAMA Ophthalmol* 139 (2021):49-56.



This article is an open access article distributed under the terms and conditions of the [Creative Commons Attribution \(CC-BY\) license 4.0](https://creativecommons.org/licenses/by/4.0/)